DOI: 10.1002/ejic.201001121

Transition-Metal Complexes Based on a Sulfonate-Containing N-Donor Ligand and Their Use as HIV Antiviral Agents

Sandra García-Gallego,[a][‡] M. Jesús Serramía,[b][‡] Eduardo Arnaiz,[a] Laura Díaz,[b] M. Angeles Muñoz-Fernández,*[b] Pilar Gómez-Sal,[c] M. Francesca Ottaviani,[d] Rafael Gómez,*[a] and F. Javier de la Mata*[a]

Keywords: Inhibitors / Antiviral agents / Transition metals / N,O ligands / HIV

Herein, we describe the synthesis and characterization of a sulfonate-containing N-donor ligand in its sodium salt and acid forms, $Na_2[(DES)MeN(CH_2)_2NMe(DES)]\cdot 2H_2O$ (**1**) and $[(DES)MeN^+H(CH_2)_2N^+HMe(DES)]\cdot H_2O$ (**2**), and its corresponding metal complexes, $[\{(DES)MeN(CH_2)_2NMe(DES)\}M(H_2O)_2]\cdot nH_2O$ [M = Ni (**3**), Co (**4**), Cu (**5**) and Zn (**6**)]. Treatment of HIV-infected MT-2 cells with Ni, Co and Cu complexes inhibit virus replication up to 50–70 % both in pre- and post-infected cells as a result of dual preventive and therapeutic behaviour.

Introduction

Human immunodeficiency virus (HIV) and its associated disease (AIDS) continue to be a major public health problem worldwide with millions of people currently infected and new infections on the rise. Highly active anti-retroviral therapy (HAART) has made AIDS more manageable despite its severe side-effects and the fact that patients remain infectious. In addition, the high mutation rate of HIV makes multiple drug resistance a continuing and challenging problem[1] with no effective vaccines available for the prevention of HIV infection so far. Therefore new lead compounds with new mechanisms of action are heavily pursued, and alternative therapies need to be explored.

There are several steps in the replicative cycle of HIV that may be considered as targets for chemotherapeutic purposes: (i) adsorption and cell fusion, (ii) reverse transcription, (iii) proviral DNA integration, (iv) proviral DNA transcription to viral mRNA, (v) viral mRNA translation to viral proteins and (vi) maturation and budding.[2] The initial events of HIV infection have been shown to be points of attack for some metal complexes, this approach being promising for the development of new anti-HIV drugs.[3] With respect to the adsorption and fusion steps, different entry and fusion inhibitors have been designed to interfere with different parts of this process. When HIV attaches to the cell surface, a specific part of the HIV envelope, a glycoprotein called gp120, binds to the CD4 cell receptor with the help of the cell co-receptors CXCR4 and CCR5 at the outer cell membrane. Metal complexes that interfere with the viral glycoprotein and/or cell receptors are currently based on polyanionic ligands (polysulfates, polysulfonates, polycarboxylates, polyoxometallates and sulfonated or carboxylated metalloporphyrins)[3] or bicyclam ligands.[4] Of the polyanionic substances, the sulfonates are good candidates for topical microbicides in the prevention of sexually transmitted diseases such as AIDS. For instance, (2-mercaptoethanesulfonato)platinum or -palladium complexes act as inhibitors of HIV-1, exhibiting antiviral activity similar to that shown by dextran sulfate.[5] Sulfonated naphthylporphyrins and their copper and iron chelates[6] and (sulfonated triazine)platinum complexes,[7] in which the sulfonated groups are not directly bonded to the transition metal atom, have also shown good potential as microbicides. Another approach involves the use of bicyclam ligands like AMD3100, which is extremely specific in its affinity for the CXCR4 co-receptor although this behaviour can be enhanced by coordination to Cu^{2+}, Zn^{2+} or Ni^{2+} metal ions.[8] Metal complexes have also been found to target other sensitive parts of the viral cycle like HIV transcriptase reverse, integrase or protease enzymes.[9]

[a] Departamento de Química Inorgánica, Universidad de Alcalá, Campus Universitario, Edificio de Farmacia, Networking Research Center on Bioengineering, Biomaterials and Nanomedicine (CIBER-BBN),
28871 Alcalá de Henares, Spain
Fax: +34-91-885-4683
E-mail: rafael.gomez@uah.es
[b] Laboratorio de Inmunobiología Molecular, Hospital General Universitario Gregorio Marañón, Madrid, Networking Research Center on Bioengineering, Biomaterials and Nanomedicine (CIBER-BBN),
Marañón, Madrid, Spain
E-mail: mmunoz.hgugm@salud.madrid.org
[c] Departamento de Química Inorgánica, Universidad de Alcalá, Campus Universitario,
28871 Alcalá de Henares, Spain
[d] Department of Geological Sciences, Chemical and Environmental Technologies,
61029 Urbino, Italy
[‡] Both authors contributed equally to this work.
Supporting information for this article is available on the WWW under http://dx.doi.org/10.1002/ejic.201001121.

Herein, we describe the synthesis and characterization of a sulfonate-containing N-donor ligand in its acid and sodium salt forms and its corresponding metal (Ni, Co, Cu and Zn) complexes in order to combine the potential cooperative effect between the sulfonate groups and the metal centre in the treatment against HIV.

Results and Discussion

Synthesis and Characterization

We synthesised the sodium salt of the ligand *N*,*N*′-dimethylethylenediamino-*N*,*N*′-diethanesulfonic acid [(DESH)-MeN(CH_2)$_2$NMe(DESH)] (DES = diethanesulfonate). The synthesis was based on the method developed by Liang et al. using a Michael-type addition reaction.[10] The conjugate addition of the secondary amine *N*,*N*′-dimethylethylenediamine to sodium vinylsulfonate in aqueous solution in a 1:2 ratio at room temperature for 12 h led to the formation of the compound Na_2[(DES)MeN(CH_2)$_2$NMe(DES)]·2H_2O (**1**) as a white solid in 88% yield, as determined from its analytical data (see Scheme 1).

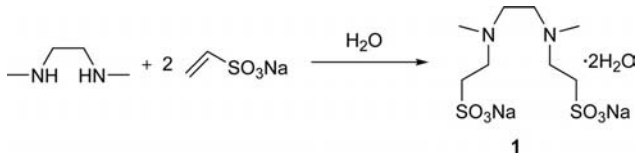

Scheme 1. Synthesis of compound Na_2[(DES)MeN(CH_2)$_2$NMe-(DES)]·2H_2O (**1**).

Compound **1** is very soluble in water, slightly soluble in methanol or ethanol and insoluble in organic solvents.

The addition of 1 equiv. of H_2SO_4 or 2 equiv. of HCl to an aqueous solution of **1** led to the precipitation of the formally zwitterionic ligand [(DES)MeN$^+$H(CH_2)$_2$N$^+$HMe-(DES)]·H_2O (**2**) as a white crystalline solid in quantitative yield (see Scheme 2), based on elemental analysis. Analogous systems have been reported elsewhere.[11] Compound **2** is soluble in hot water, but insoluble in methanol, ethanol and organic solvents.

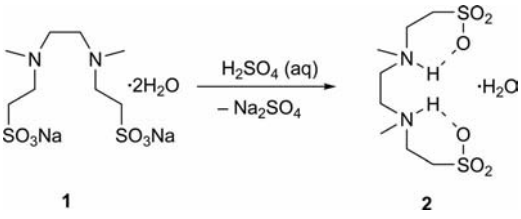

Scheme 2. Synthesis of compound [(DES)MeN$^+$H(CH_2)$_2$N$^+$-HMe(DES)]·H_2O (**2**).

Complexes **1** and **2** were fully characterized by analytical and NMR spectroscopic data (see the Exp. Sect. and the Supporting Information).

The protonation behaviour of compound **1** depending on the pH of the medium was studied by potentiometric titration in pure distilled water of no ionic strength. The system presents two equivalent tertiary amines and two sulfonate groups with pronounced differences in their protonation processes. In fact, the titration curve displays two pK_a values at 4.6 (pK_{a1}) and 9.7 (pK_{a2}), which correspond to the two acidic dissociation constants of the ammonium groups (see Figure 1 and the Exp. Sect.), whereas pK_a values for the sulfonate group were not observed, as expected.

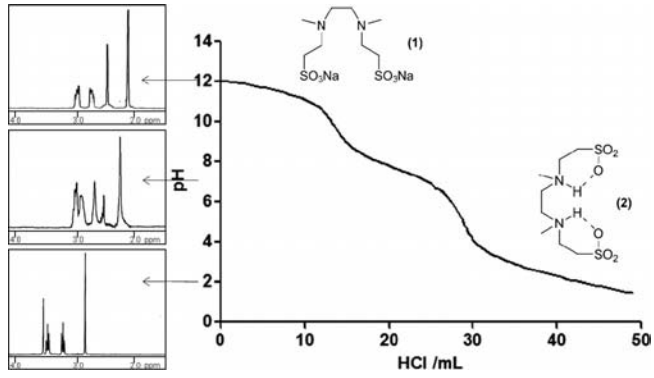

Figure 1. Titration curve of compound **1** and ^{1}H NMR spectra at pH = 12, 7 and 2.

Similar values have been observed for analogous systems like zwitterionic *N*-substituted aminosulfonic acid buffers referred to as Good's buffers.[12] The values mean that at pH > 9.7 the main species would be the dianionic form [(DES)MeN(CH_2)$_2$NMe(DES)]$^{2-}$, analogous to compound **1**, whereas at pH < 4.6 the zwitterionic form would be the prevailing form. However, compounds **1** and **2** show completely different coordination behaviour to that of Good's buffers, which show weak to non-existent complexation properties (see below).

Compounds **1** and **2** were used to synthesize transition-metal complexes based on Ni, Co, Cu and Zn. Treatment of **1** with 1 equiv. of $NiBr_2$·3H_2O in water cleanly afforded a turquoise-green precipitate of [{(DES)MeN(CH_2)$_2$NMe-(DES)}Ni(H_2O)$_2$]·2H_2O (**3**) in 90% yield, based on a quantitative analysis (see Scheme 3). This is an air-stable compound, slightly soluble in water but soluble in alcohols and DMSO. Single crystals of **3** suitable for X-ray diffraction studies were obtained by recrystallization from ethanol or methanol, which confirmed its stoichiometry. Compound **3** was prepared previously by Reedijk and co-workers by an oxidation of a mononuclear nickel dithiolate complex with hydrogen peroxide and was characterized by single-crystal X-ray crystallography.[13] The UV/Vis spectrum of complex **3** was also recorded and presents bands at λ_{max} = 649 and 383 nm in water very close to those observed at λ_{max} = 653 and 386 nm by solid-state reflectance reported by Reedijk and co-workers.[13]

The analogous reaction with $CoCl_2$ led to the formation of a pink solution, and concentration of the aqueous solution afforded pink microcrystals of [{(DES)MeN(CH_2)$_2$-NMe(DES)}Co(H_2O)$_2$]·2H_2O (**4**) in 80% yield, as determined by quantitative analysis and X-ray diffraction studies (see below). Again, the cobalt complex is air-stable, slightly

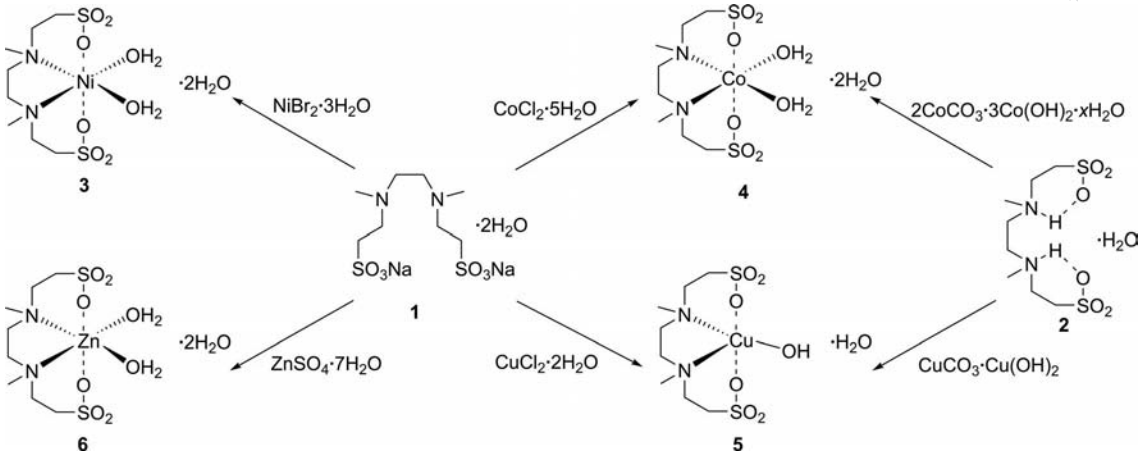

Scheme 3. Synthesis of compounds **3**–**6** by starting from **1** or **2**.

soluble in water and alcohols and soluble in DMSO. Both the nickel and cobalt complexes were separated from the alkali halides, NaBr or NaCl, respectively, by means of their different water solubilities. Alternatively, complex **4** can be cleanly prepared from the zwitterionic form **2** and the mixed cobalt derivative $[2Co(CO_3)\cdot 3Co(OH)_2]\cdot xH_2O$ in almost quantitative yield. The poor solubility of complex **4** prevented the acquisition of an accurate UV/Vis spectrum in solution. However, elemental analysis of microcrystal samples produced from the two different synthetic procedures confirmed the formation of the same cobalt complex.

In the case of copper, the addition of 1 equiv. of $CuCl_2$ to the disodium salt **1** in water afforded a dark-blue solution which did not show any precipitate because of the high solubility of the corresponding copper coordination complex. The use of a water/methanol double layer gave rise to blue crystals in 78% yield corresponding to the compound $[\{(DES)MeN(CH_2)_2NMe(DES)\}Cu(H_2O)]\cdot H_2O$ (**5**), again as determined by analytical data and X-ray diffraction studies (see below). The complex is air-stable, very soluble in water and DMSO and slightly soluble in methanol or ethanol. Similarly to derivative **4**, complex **5** was cleanly synthesized from **2** and $[Cu(CO_3)\cdot Cu(OH)_2]$ in quantitative yield avoiding the formation of an alkali halide as a side-product. The spectroscopic and analytical data of samples produced by the two different synthetic approaches confirmed the formation of the same copper complex. Compound **5** absorbs in water at λ_{max} = 278 (ε = 3770 $M^{-1}cm^{-1}$) and 684 nm (ε = 73 $M^{-1}cm^{-1}$). The former value can be ascribed to a charge-transfer band (MLCT or LMCT), whereas the latter is due to a d→d transition, which indicates that the geometry around the copper atom in solution is intermediate between a square pyramid (absorption maximum 526–625 nm) and a trigonal bipyramid (absorption maximum 666–1000 nm).[14,15] However, a pseudo-octahedral structure cannot be ruled out in solution because an "N_2O_4" ligand should absorb between the strong-field "N_6" ligand (578 nm) as in $[Cu(1\text{-allylimidazole})_6]^{2+}$,[16,17] and "$O_6$" ligand (794 nm) as in $[Cu(H_2O)_6]^{2+}$.[16] To confirm that complex **5** is sufficiently stable at physiological pH, UV/Vis spectra were recorded at different pHs (see Figure 2). Complex **5** dissolved in pure distilled water afforded a pH of 5.75, which means that both aqua and hydroxido species are present. The UV/Vis spectra recorded at different pHs are shown in Figure 2; note that complex **5** is stable enough in the range 9–4 and therefore at physiological pH. Above or below this range, the charge-transfer band disappears and a bathochromic effect of the d→d band is observed showing decomplexation presumably due to the formation of $Cu(OH)_2$ or $[Cu(H_2O)_6]^{2+}$, respectively. Another feature is the observation of a buffer effect on the pH as a result of the equilibrium of the aqua and hydroxido forms of complex **5**.

The UV/Vis spectra of a mixture of the Cu^{2+} cation and compound **1** at different ratios (metal/compound **1**: 1:5, 1:2 and 1:1) show a shifting of the absorption to higher λ_{max} values on increasing the amount of copper consistent with the presence of more O atoms in the coordination sphere and thus with only one ligand per metal atom in a ratio of 1:1. Thus, the possibility of ligand exchange to give a 1:2 complex may be excluded when complex **5** is in solution. In addition, the band due to the free copper cation is never observed.

EPR spectroscopy was used to gain additional information on the Cu coordination in compound **5** in aqueous solution. The magnetic parameters indicate that the complex geometry is square-planar, which is consistent with the square-pyramidal geometry observed in the crystal structure (see below) if we assume an elongation in the axial direction. The EPR magnetic parameters of compound **5** (Figure 3) obtained from simulation of the spectral lineshape at room temperature (298 K) are $<g>$ = 2.157 and $<A>$ = 62.1 G. At low temperature (150 K), the EPR spectra of **5** show a poor resolution, and the anisotropic values were roughly evaluated ($g_{\|} \approx 2.29$, $A_{\|} \approx 160$ G) and are similar to those found for Cu^{II} complexes formed with carboxylate-terminated PAMAM dendrimers with a CuN_2O_2 coordination mode ($<g>$ = 2.130 and $<A>$ = 68 G; $g_{\|}$ = 2.265, $A_{\|}$ = 170 G).[18] Similar magnetic parameters have

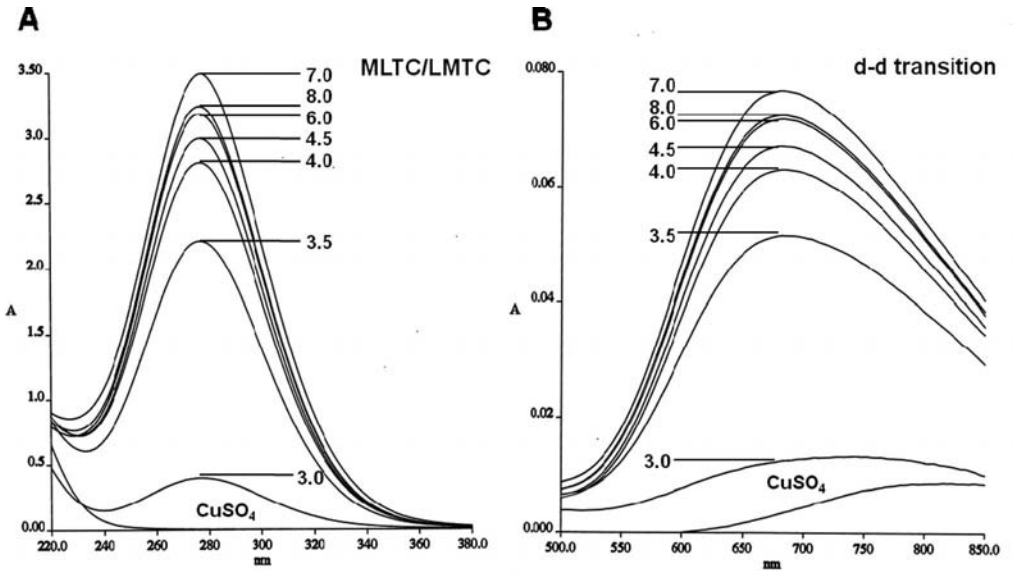

Figure 2. UV/Vis spectra of compound **5** recorded at different pH values. (A) Charge-transfer band at 278 nm. (B) d→d transition band at 684 nm.

been reported in the literature for several copper complexes.[19] The lower values of $<A>$ and $A_{\parallel}$ (and the corresponding increase in $<g>$ and $g_{\parallel}$) observed in **5** compared with those shown by Cu^{II}–0.5 G-PAMAM can be accounted for the presence of a stronger Cu–O bonding in the Cu–OSO_2R fragment compared to the COO–Cu unit.

The EPR spectra recorded in the presence of the Cu ion and the sodium salt **1** at different molar ratios (metal/compound **1**: 1:1, 1:2 and 1:5) revealed different spectroscopic parameters. At the lowest Cu concentration (1:5 ratio), the higher $A_{\parallel}$ (176 G) and lower $g_{\parallel}$ (2.241) values indicate an increased electron density on the copper atom, which in turn indicates that the nitrogen atoms are involved in the metal coordination more efficiently than the negatively charged oxygen atoms and is consistent with the existence of more than one ligand molecule. On increasing the copper concentration (for a 1:2 ratio, $A_{\parallel}$ = 166 G and $g_{\parallel}$ = 2.260, whereas for a 1:1 ratio the same values as for compound **5** were observed), a shift to lower values of the hyperfine constant is consistent with more coordinated oxygen atoms around the metal atom and again with the presence of a one ligand molecule in a ratio of 1:1. This feature is in agreement with the UV/Vis data mentioned before for the same experiment.

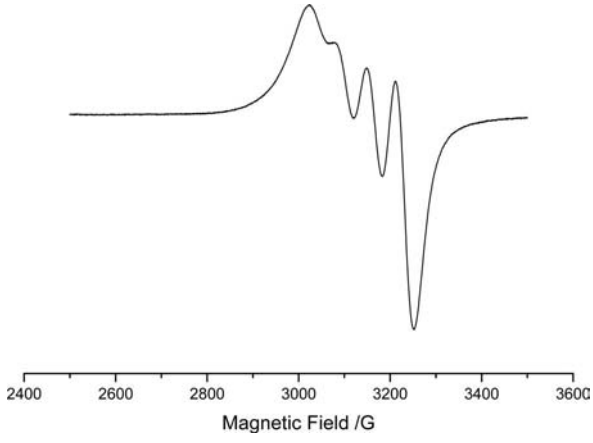

Figure 3. EPR spectrum of compound **5**, recorded at 298 K.

Finally, treatment of **1** with 1 equiv. of $ZnSO_4 \cdot 7H_2O$ in water led to a white solid of [{(DES)MeN$(CH_2)_2$-NMe(DES)]}$Zn(H_2O)_2]\cdot 2H_2O$ (**6**) in 45% yield. This derivative is air-stable and partially soluble in water. The ^{1}H NMR spectrum shows a broad singlet at δ = 3.04 ppm for both the –NCH_2CH_2N– and the –$CH_2CH_2SO_3Na$ groups; another signal for the –$CH_2CH_2SO_3Na$ group appears as a broad singlet at δ = 2.89 ppm. Finally, the MeN group provides a singlet at δ = 2.42 ppm. Four resonances were observed in the ^{13}C NMR spectrum and assigned on the basis of HMQC and HMBC experiments (see Exp. Sect.). The signals at δ = 40.3 and 46.2 ppm have been attributed to the MeN– and the –NCH_2CH_2N– groups, respectively, whereas the resonances at δ = 51.6 and 51.8 ppm are due to both methylene groups of –$NCH_2CH_2SO_3^-$.

X-ray Structural Analyses

The structures of complexes **4**–**6** were determined by single-crystal X-ray diffraction techniques. Selected bond lengths and angles for the three complexes are provided in Table 1, labelled representations of their molecular structures are shown in Figure 4, and the crystal data are shown in Table 2.

For the complexes **4** and **6**, the coordination around the metal centre is octahedral with the metal atom sitting on a crystallographic two-fold axis; thus, the asymmetric unit in the unit cell is only half a molecule. The aminosulfonato ligand occupies four coordination sites with the amine ni-

Table 1. Selected bond lengths [Å] and angles [°] for **4**, **5** and **6**.[a]

	M = Co (**4**)	M = Zn (**6**)	M = Cu (**5**)	
M–O(1)	2.085(2)	2.0984(18)	Cu(1)–O(1)	2.235(4)
M–O(1^{i})	2.085(2)	2.0984(18)	Cu(1)–O(4)	1.985(4)
M–O(4)	2.147(2)	2.1202(18)	Cu(1)–O(7)	2.028(4)
M–N(1)	2.223(3)	2.206(2)	Cu(1)–N(2)	2.054(5)
			Cu(1)–N(1)	2.055(5)
O(1^{i})–M–O(1)	172.66(13)	171.66(10)	O(4)–Cu(1)–O(1)	90.49(17)
O(1)–M–O(4^{i})	85.01(9)	84.65(7)	O(4)–Cu(1)–N(1)	175.89(19)
O(1)–M–O(4)	89.88(9)	89.56(7)	O(4)–Cu(1)–N(2)	89.62(18)
O(4^{i})–M–O(4)	91.70(13)	92.16(11)	O(7)–Cu(1)–N(2)	161.27(19)
O(1^{i})–M–N(1^{i})	95.11(10)	95.73(8)	O(4)–Cu(1)–O(7)	91.83(19)
O(1)–M–N(1^{i})	90.38(9)	90.47(7)	N(2)–Cu(1)–N(1)	86.44(19)
O(4)–M–N(1)	92.73(10)	92.16(8)	O(7)–Cu(1)–O(1)	94.08(17)
O(1)–M–N(1)	95.11(10)	95.73(8)	N(1)–Cu(1)–O(1)	91.65(18)
O(4)–M–N(1^{i})	173.60(10)	173.46(8)	O(7)–Cu(1)–N(1)	91.52(19)
N(1^{i})-M–N(1)	83.24(15)	83.98(12)	N(2)–Cu(1)–O(1)	104.58(18)

[a] Symmetry transformations used to generate equivalent atoms: M = Co: (i) $-x$, y, $-z + {}^{3}/_{2}$; M = Zn: (i) $-x$, y, $-z + ½$.

trogen atoms located in *cis* positions and the two sulfonate oxygen atoms in *trans* positions. The octahedral environment is completed by two water molecules *cis* to each other. In addition, another two non-coordinated water molecules are found for each molecule of the complex. In complex **4**, the Co–N bond lengths 2.223(3) Å are in the expected range for octahedrally coordinated cobalt[16,20] and are longer than the Co–O bond lengths. In our case, the Co–O bonds corresponding to the two sulfonate oxygen atoms in *trans* positions are 2.085(2) Å, shorter than those of the coordinated water ligands, which are 2.147(2) Å. These distances are in the expected range found for related "N_2O_4" complexes.[20] The N(1)–Co–N(1^{i}) angle is 83.24(15)°, smaller than the ideal 90° probably as a result of the chelate effect, whereas the other angles in the equatorial plane, N(1)–Co–O(4), O(1)–Co–O(4) and O(4)–Co–O(4^{i}), are obtuse. Finally, the N(1)–Co–O(4^{i}) angle is 172.66 (13)°.

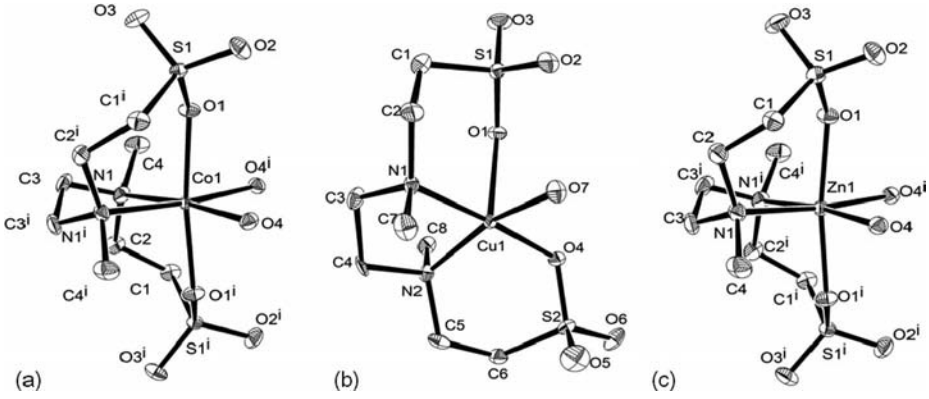

Figure 4. ORTEP plots (50% probability ellipsoids) of the single-crystal X-ray structures of (a) **4**, (b) **5** and (c) **6**.

Table 2. Crystal data for the single-crystal X-ray structures of complexes **4**–**6**.

	4	**5**	**6**
Empirical formula	$C_8H_{26}N_2CoO_{10}S_2$	$C_8H_{22}N_2CuO_8S_2$	$C_8H_{26}N_2O_{10}S_2Zn$
M_r	433.36	401.94	439,80
Crystal system	monoclinic	monoclinic	monoclinic
Space group	*C*2/*c*	$P2_1/n$	*C*2/*c*
a [Å]	14.636(3)	6.7947(3)	14.595(3)
b [Å]	9.6560(10)	23.313(5)	9.5169(18)
c [Å]	12.639(2)	10.547(2)	12.6644(9)
β [°]	101.31(2)	106.340(7)	101.40(1)
Volume [Å^3]	1751.5(5)	1603.2(5)	1724.4(5)
Z	4	4	4
Density (calcd.) [Mg m^{-3}]	1.643	1.665	1.694
μ [mm^{-1}]	1.267	1.659	1.716
T [K]	200(2)	200(2)	200(2)
Crystal size	0.5 × 0.4 × 0.4.	0.4 × 0.3 × 0.2	0.4 × 0.4 × 0.25
θ range [°]	3.18–27.53	3.21–27.51	3.20–27.51
Measured reflections	13814	31914	18795
Unique reflections (R_{int})	3854 (0.0837)	3676 (0.1349)	1988 (0.1282)
θ [°], completeness (%)	27.53, 97.0	27.51, 99.7	27.51, 99.7
Goodness-of-fit on F^2	1.284	1.178	1.235
*R*1, *wR*2 [$I > 2\sigma(I)$]	0.0430, 0.1128	0.0719, 0.1736	0.0381, 0.0945
*R*1, *wR*2 (all data)	0.0534, 0.1383	0.0933, 0.1873	0.0480, 0.1131
Absorption coefficient [mm^{-1}]	1.267	1.659	1.716
Largest diff. peak, hole [e Å^{-3}]	0.774, –1.609	2.806, –1.523	0.773, –1.532

The zinc complex **6** has the same geometry as that shown by complex **4** with the normal variations in bond lengths and angles due to the presence of a different metal. The Zn–N bond length is 2.206(2) Å, also in the expected range for octahedrally coordinated zinc,[16,20,21] and is again longer than the Zn–O bonds. The angles are very similar to those of derivative **4**.

Regarding the copper complex **5**, this can be described as a square pyramid in which the O1 atom is in the apical position and the other donor atoms in the square plane. Angles of the *cis*-bonded atoms range from 86 to 91.83° in the square plane and from 91.65 to 104.5° with the apical atom. The Cu–N bond lengths are practically identical [2.055(5) and 2.054(5) Å] for both nitrogen atoms. The Cu–O bond lengths are similar for both equatorial oxygen atoms: one formed with the sulfonate oxygen atom Cu–O(4), 1.984(4) Å, and the other with a water molecule Cu–O(7), 2.028(4) Å. However, the other sulfonate oxygen bond Cu–O(1), located in the apical position is longer [2.235(4) Å], which supports the description of the molecule as a square pyramid in the solid state. The Cu–N and Cu–O bond lengths are in the expected range for pentacoordinate copper complexes.[22]

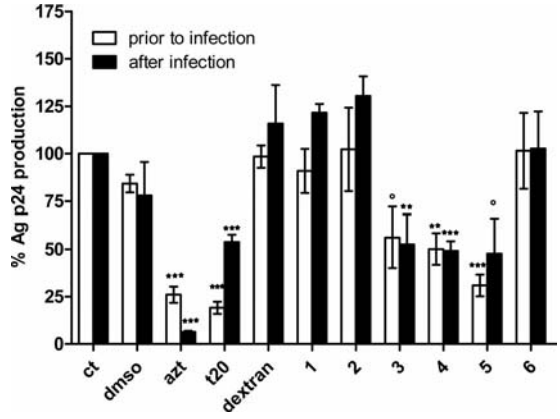

Figure 5. ELISA assay for the viral protein p24 antigen at 48 h pre- and post-treatment. White bars denote pre-treatment, and black bars denote post-treatment. Differences from the control group were statistically analyzed (°$p < 0.2$, **$p < 0.05$, ***$p < 0.01$). The results are the mean of three different experiments. AZT (inhibitor of retrotranscription, at a concentration of 0.5 μM) and T-20 (fusion inhibitor, 15 μM) were used as positive controls of the viral inhibition. A concentration of 5 μM of dextran, which does not affect the viral infection, was used as a control.

Biological Assays

Complexes **1**–**5** were not toxic towards MT-2 cells in the measurement of biocompatibility by the MTT test in the range 0.5–5 μM for 24 h. However, complex **6** did exhibit some degree of toxicity (see the Supporting Information).

HIV Inhibition Assays

Compounds **1**–**6** were evaluated for HIV antiviral activity. In the first experiment, the pre-treatment of the MT-2 cells with compounds **1**–**6** prior to HIV infection were studied (preventive behaviour). Cells were incubated with compounds **1**–**6** at 5 μM for 2 h. Afterwards, these cells were infected with HIV NL4.3 for 2 h, and after 48 h the supernatant was collected and the production of Ag p24 measured. The results are shown in Figure 5 and reveal an HIV inhibition of 45 and 50% for compounds **3** and **4**, respectively, whereas 70% inhibition was observed for **5**; all are compared with mock treated cells (see white bars). However, no HIV inhibition was observed when the MT-2 cells were pre-treated with 5 μM **1**, **2** or **6** compared with the mock treated MT-2 cells. This fact reveals that the ligand is not active in aminosulfonated disodium salt or zwitterionic forms. After 48 h of treatment, cell viability was also determined by flow cytometry, and no toxicity was detected up to 5 μM for compounds **1**–**6** in the treatment (see the Supporting Information), which indicates that the inhibition observed by **3**–**5** is not associated with cytotoxicity effects.

To discriminate between a putative effect attributed to the non-complexed metal ion and that of the complex itself, the inhibitory efficiencies of complex **4** or **5** and $CoCl_2$ and $CuCl_2$, respectively, were compared under the same experimental conditions. As shown in Figure 6, at 5 μM, $CoCl_2$ presents an inhibition of 18% compared with an inhibition of 55% for complex **4**, whereas $CuCl_2$ displays an inhibition of 33% against an inhibition of more than 60% for complex **5** under the experimental conditions. Note that when the inhibition experiment was performed at 2 μM, no inhibition effect was observed for $CuCl_2$, whereas complex **5** almost maintained its efficiency (57% inhibition, data not shown). These results clearly indicate that ligand coordination to the metal centre enhances its inhibitory activity and confirm that the complexes are stable enough under the experimental conditions of the assay.

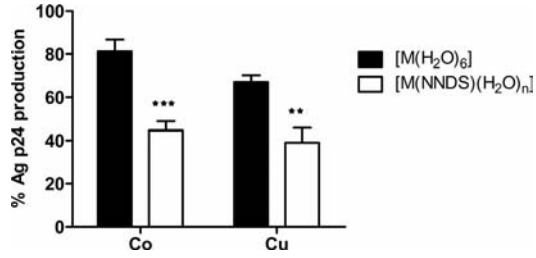

Figure 6. ELISA assay for the viral protein p24 antigen after 48 h of pre-treatment. Inhibitory activity of compounds **4** and **5** and $CoCl_2$ and $CuCl_2$ at 5 μM. The differences between groups were statistically analyzed (**$p < 0.05$, ***$p < 0.01$).

In a second experiment, MT-2 cells were first infected for 2 h with HIV NL4.3 and then treated with 5 μM of **1**–**6** for 48 h, after which the supernatant was collected and the production of Ag p24 was measured (therapeutic behaviour). Results showed around 50% HIV inhibition for complexes **3**–**5** compared with mock treated cells (see Figure 5). Again, no inhibition was observed with **1**, **2** and **6** in the post-treatment experiment. In addition, no cell toxicity was detected by flow cytometry during this experiment (data not shown).

Conclusions

A new aminosulfonato ligand has been prepared and used in the synthesis of transition-metal complexes based on nickel, cobalt, copper and zinc. Compounds **1** and **2** were observed to have completely different coordination behaviour to Good's buffers, which show weak to non-existent complexation properties. All the metal complexes show a pseudo-octahedral environment in the solid state, except the copper complex, which is better described as a square pyramid in the solid state and is roughly consistent with that observed in solution by UV/Vis and EPR measurements. It is worth highlighting that the aminosulfonato ligand in its sodium salt form **1**, as the core of the metallic complexes, is not toxic and shows no inhibitory effects against HIV, either in pre-infected or post-infected MT-2 cells. Treatment with nickel and cobalt complexes inhibits HIV replication by around 50% in both pre- and post-infected cells. In the case of the copper complex, 70% inhibition in the pre-infected cells and more than 50% in the post-infected cells were observed.

Because complexes **3**–**5** showed anti-HIV activity in the pre-infected cell experiment, this feature may be indicative of fusion inhibitor activity. However, when the treatment was administrated after cell infection, compounds **3**–**5** were also found to be capable of inhibiting HIV replication, which indicates that they may also act in subsequent steps of the replicative cycle. This dual behaviour may be considered the greatest characteristic of these compounds as they combine HIV preventive and therapeutic behaviour in a single molecule. In this sense, this family of complexes may be considered as promising new lead compounds for the development of targeted anti-virals.

Experimental Section

General Methods: Unless otherwise stated, reagents were obtained from commercial sources and used as received. ^{1}H, ^{13}C and ^{15}N NMR spectra were recorded with Varian Unity VXR300 and 500 Plus instruments. Chemical shifts (δ) were measured relative to residual ^{1}H for [D_2]water used as solvent. For ^{13}C and ^{15}N NMR, external references were used (tetramethylsilane and nitromethane, respectively). C, H and N analyses were carried out with a Perkin–Elmer 240 C microanalyzer and UV/Vis analyses with a Perkin–Elmer Lambda 18 UV/Vis spectrophotometer. The EPR spectra were recorded with an EMX-Bruker spectrometer operating in the X band (9.5 GHz), and simulations of the spectra to evaluate the magnetic parameters (accuracy 5%) were performed with the program WINEPR SimFonia, version 1.25 (Bruker) and with the program CU23G.[23] The temperature was controlled with a Bruker ST3000 variable-temperature assembly. The potentiometric titrations were performed by using a CRISON titration system consisting of a digital potentiometer (pH-Meter BASIC 20+) and a pH electrode, which has an encapsulated reference system (cartridge) with an Ag^+ ion barrier, two diaphragms and CRISOLYT electrolyte. The pH meter was standardized at pH = 4.01, 7.00 and 9.21 by using the appropriate buffer solutions. The titration was carried out with 60 mg of compound **1** and 0.0105 M HCl solution. The pK_a values were calculated by using the second-derivative method.[24]

Synthesis of Na_2[(DES)MeN$(CH_2)_2$NMe(DES)]·$2H_2O$ (1): *N*,*N*′-Dimethylethylenediamine (1.51 mL, 14.18 mmol) and sodium vinylsulfonate (10.4 mL, 28.36 mmol) were mixed in an ampoule. The resulting solution was stirred at 120 °C for 12 h and then concentrated under reduced pressure. The resulting product was washed with Et_2O (3 × 5 mL) and dried under vacuum to give **1** as a white water-soluble solid (5.32 g, 98%). ^{1}H NMR (D_2O): δ = 2.87 (2 m, 4 H, –$NCH_2CH_2SO_3Na$), 2.70 (2 m, 4 H, –$NCH_2CH_2SO_3Na$), 2.42 [s, 4 H, –$N(CH_2)_2N$–], 2.07 (s, 6 H, –NCH_3) ppm. ^{13}C NMR (D_2O): δ = 53.0 [–$N(CH_2)_2N$–], 51.6 (–$NCH_2CH_2SO_3Na$), 47.3 (–$NCH_2CH_2SO_3Na$), 41.0 (–NCH_3) ppm. ^{15}N NMR (D_2O): δ = –349 ppm. $C_8H_{22}N_2Na_2O_8S_2$ (384.4): calcd. C 25.00, H 5.77, N 7.29, S 16.68; found C 24.84, H 5.27, N 6.83, S 16.91.

Synthesis of [(DES)MeN$^+$H$(CH_2)_2$N$^+$HMe(DES)]·H_2O (2): The addition of 1 equiv. of H_2SO_4 (0.14 mL, 2.6 mmol) to an aqueous solution (5 mL) of **1** (1 g, 2.6 mmol) and subsequent stirring for 1 h led to the precipitation of a white solid. The solid was isolated by filtration and purified by recrystallization from hot water to give **2** as white microcrystals (0.96 g, 100%). ^{1}H NMR (D_2O): δ = 3.48 (2 m, 4 H, –$NCH_2CH_2SO_3Na$), 3.20 (2 m, 4 H, –$NCH_2CH_2SO_3Na$), 3.57 [s, 4 H, –$N(CH_2)_2N$–], 2.84 (s, 6 H, –NCH_3) ppm. ^{13}C NMR (D_2O): δ = 52.6 (–$NCH_2CH_2SO_3Na$), 44.8 (–$NCH_2CH_2SO_3Na$), 50.0 [–$N(CH_2)_2N$–], 41.0 (–NCH_3) ppm. ^{15}N NMR (D_2O): δ =–337 ppm. $C_8H_{22}N_2O_7S_2$ (322.4): calcd. C 29.80, H 6.88, N 8.69, S 19.89; found C 29.42, H 6.36, N 8.61, S 20.31.

Synthesis of [{(DES)MeN$(CH_2)_2$NMe(DES)}Ni$(H_2O)_2$]·$2H_2O$ (3): An aqueous solution (2 mL) of $NiBr_2·3H_2O$ (0.42 g, 1.56 mmol) was added to an aqueous solution (5 mL) of **1** (0.6 g, 1.56 mmol). The mixture was stirred for 2 h to assure completion of the reaction, and the resulting product was filtered, washed with H_2O (1 × 4 mL) and finally dried under vacuum. Compound **3** was obtained as a turquoise-green solid (0.61 g, 94%). Crystals suitable for X-ray diffraction studies were obtained by recrystallization from water. $C_8H_{24}N_2NiO_9S_2$ (414.03): calcd. C 22.18, H 6.05, N 6.47, S 14.81; found C 22.17, H 5.71, N 6.34, S 14.51. UV/Vis (H_2O): λ_{max} = 383 nm, 649 nm.

Synthesis of [{(DES)MeN$(CH_2)_2$NMe(DES)}Co$(H_2O)_2$]·$2H_2O$ (4)

Method 1: This compound was prepared by using a similar method to that described for **3**, starting from **1** (0.60 g, 1.56 mmol) and $CoCl_2·5H_2O$ (0.34 g, 1.56 mmol). The pink solution obtained after 2 h of reaction was concentrated under reduced pressure and cooled to 10 °C. The precipitate was filtered, washed with ethanol and dried under vacuum. Compound **4** was isolated as a pink solid (80%), scarcely soluble in water.

Method 2: Complex **4** can also be synthesized by starting from an aqueous solution (10 mL) of **2** (100 mg, 0.33 mmol) and an aqueous solution (5 mL) of $2CoCO_3·3Co(OH)_2·xH_2O$ (50% weight on Co; 39 mg, 0.33 mmol on cobalt). The mixture was stirred overnight and the resulting precipitate filtered, washed with ethanol and dried under reduced pressure to give **4** in 100% yield (143 mg) without any byproduct. Crystals suitable for X-ray diffraction studies were obtained by recrystallization from water. $C_8H_{26}CoN_2O_{10}S_2$ (433.36): calcd. C 22.17, H 6.05, N 6.46, S 14.80; found C 21.77, H 6.04, N 6.42, S 14.77.

Synthesis of [{(DES)MeN$(CH_2)_2$NMe(DES)}Cu(H_2O)]·H_2O (5)

Method 1: Compound **5** was prepared according to the same procedure as that described for compounds **3** and **4**. An aqueous solution (5 mL) of **1** (0.6 g, 1.56 mmol) and an aqueous solution (5 mL) of $CuCl_2·2H_2O$ (0.26 g, 1.56 mmol) were mixed, and the resulting solution was stirred for 2 h and then concentrated under reduced pressure. Compound **5** was obtained by precipitation in a water/

methanol double layer and isolated as a dark-blue solid after drying it under reduced pressure (0.54 g, 78%).

Method 2: Compound **5** can also be synthesized by starting from an aqueous solution (10 mL) of **2** (100 mg, 0.33 mmol) and an aqueous solution (5 mL) of $CuCO_3{\cdot}Cu(OH)_2$ (36 mg, 0.16 mmol). The mixture was stirred overnight, filtered and concentrated under reduced pressure until dryness to give **5** in 100% yield (132 mg) without any byproduct. $C_8H_{22}CuN_2O_8S_2$ (401.94): calcd. C 23.91, H 5.52, N 6.97, S 15.95; found C 23.67, H 5.47, N 7.11, S 15.98. UV/Vis (H_2O): λ_{max} (ε) = 278 (3370), 684 nm (73 $M^{-1}cm^{-1}$). EPR data (298 K): $<g>$ = 2.157 and $<A>$ = 62.1 G; (low temperature): $g_{\|} \approx 2.29$, $A_{\|} \approx 160$ G. Crystals suitable for X-ray diffraction studies were obtained by slow diffusion recrystallization in a water/methanol double layer.

Synthesis of [{(DES)MeN(CH$_2$)$_2$NMe(DES)}Zn(H$_2$O)$_2$]·2H$_2$O (6): In a similar way, $ZnSO_4{\cdot}7H_2O$ (187 mg, 0.65 mmol) dissolved in water was added to an aqueous solution (5 mL) of **1** (250 mg, 0.65 mmol). The mixture was stirred for 1 h, and a white precipitate was isolated by filtration and dried under reduced pressure (129 mg, 45%). Crystals suitable for X-ray diffraction studies were obtained by recrystallization in water. ^{1}H NMR (D_2O): δ = 3.04 [br. s, 8 H, overlapped one methylene signal of $-NCH_2CH_2SO_3Na$, indistinctly, and $-N(CH_2)_2N-$], 2.89 (br. s, 4 H, one methylene signal of $-NCH_2CH_2SO_3Na$, indistinctly), 2.42 (s, 6 H, $-NCH_3$) ppm. ^{13}C NMR (D_2O): δ = 51.8, 51.6 ($-NCH_2CH_2SO_3Na$), 46.2 [$-N(CH_2)_2N-$], 40.3 ($-NCH_3$) ppm. $C_8H_{24}N_2O_9S_2Zn$ (421.8): calcd. C 21.85, H 5.96, N 6.37, S 14.58; found C 21.69, H 5.22, N 6.39, S 15.03.

Cell Line: The established cell line MT-2 [human T-cell leukemia virus type 1 (HTLV-1)-infected cell line] was maintained in complete RPMI 1640 growth medium (Biochrom AG) supplemented with 5% fetal bovine serum (FBS), 2 mM glutamine, 1% ampicillin, 1% cloxacillin and 0.32% gentamicin at 37 °C in a 5% CO_2 atmosphere.

MTT Assay: The MTT assay shows detrimental intracellular effects on mitochondria and metabolic activity in cells. DMSO stock solutions for all compounds were prepared and then added to an aqueous solution from which the amount of DMSO was neglected (less than 0.5 μM). No precipitate was observed by using this protocol. MT-2 cells were seeded in 96-well plates in OPTIMEM® I medium containing 5% FBS (100×10^5 cells at 200 μL/well) and submitted to treatment with 5 μL of compounds **1**–**6** dissolved in water/DMSO (less than 0.5 μM): 0.5, 1, 2, 5, 10 and 15 μM. After 20 h, 20 μL of MTT [3-(4,5-dimethylthiazol-2-yl)-2,5-diphenyltetrazolium bromide] substrate solution (5 mg/mL) in water was added to the cells to measure the mitochondrial activity. After 4 h, the supernatant was removed, and the formazan crystals formed were dissolved in DMSO (200 μL per well). The concentration of formazan was then determined spectrophotometrically in a plate reader by measuring the absorbance at 550 nm. Each compound concentration was tested in triplicate according to ATCC directives.

Flow Cytometry: Following treatment with **1**–**6** before infection with the HIV-1 NL4.3 isolate, cells were analysed by flow cytometry to determine the percentage of the cell population that could be deemed viable. The cells were stained with 5 μL of propidium iodide (stock solution: 1 mg/mL; IP: Sigma) and the analysis performed with an FC 500 flow cytometer (Beckman Coulter, Hialeah, FL). Culture viability (number of dead cells as a percentage of the total number of cells) was calculated directly after appropriate gating to exclude culture debris by the instrument using the forward scatter light signal after 48 h of infection.

HIV Inhibition Experiments

Pre-Infection Assay: The MT-2 cell line was seeded at a concentration of $(1.5–2) \times 10^5$ cells/well (80000 cells/200 μL of culture medium). The cells were grown in 5% SFT RPMI culture medium. Compounds **1**–**6** were added at a concentration of 5 μM and left in the culture for 2 h. The necessary amount of virus HIV-1 NL4.3 isolate (10 ng/10^6 cells) was added to the culture and left for 2 h. Subsequently, the culture plate was centrifuged and the supernatant removed. Growth medium was added again and left in the culture for 48 h. The supernatant was collected and assayed for viral concentration by using the HIV protein p24 ELISA kit according to the kit protocol.

Post-Infection Assay: MT-2 cells were infected with HIV-1 NL4.3 isolate at a concentration of 10 ng/10^6 cells. After 2 h, MT-2 infected cells were washed twice with warm medium before being plated into 96 wells in 200 μL of RPMI culture medium with 5% SFT. Compounds **1**–**6** were added to the MT-2 infected cells within 2 h of the end of the incubation with HIV NL4.3 and left at 37 °C and under a 5% CO_2 atmosphere for 48 h. Samples were collected 48 h after treatment, spun, and the supernatant was collected and assayed for viral concentration by using the HIV protein p24 ELISA kit according to the kit protocol.

AZT (inhibitor of retrotranscription) at a concentration of 0.5 μM and T-20 (fusion inhibitor) at 15 μM were used as positive controls of the inhibition of viral infection. Dextran at a concentration of 5 μM was used as a control molecule that does not affect the viral infection.

X-ray Crystal Structure Determinations: Single crystals of **4**–**6** suitable for X-ray diffraction studies were obtained by recrystallization from water for **4** and **6**, whereas for **5** slow diffusion of a water/methanol double layer was used. A summary of the crystal data, data collection and refinement parameters for the structural analysis of each compound is given in Table 2. Suitable crystals were covered with mineral oil and mounted in the N_2 stream of a Bruker–Nonius Kappa-CCD diffractometer equipped with an area detector and an Oxford Cryostream 700 unit. Data were collected by using graphite-monochromated Mo-K_α radiation (λ = 0.71069 Å) at 200 K with an exposure time of 10 s per frame (3 sets, 230 frames, φ and ω scan, 2° scan width) for compound **4**, an exposure time of 7 s per frame (6 sets, 485 frames, φ and ω scans, 1.4° scan width) for compound **5** and an exposure time of 10 s per frame (6 sets, 306 frames, φ and ω scans, 2° scan width) for compound **6**. Raw data were corrected for Lorenztian and polarization effects. The structures were solved by direct methods, completed by subsequent difference Fourier techniques, and refined by full-matrix least squares on F^2 with SHELXL-97.[25] Anisotropic thermal parameters were used in the last cycles of refinement for the non-hydrogen atoms. Most of the hydrogen atoms were introduced into the last cycle of the refinement from geometrical calculations and refined by using a riding model. All the calculations were made by using the WINGX program.[26] CCDC-769129 (**4**), -769130 (**5**) and -769131 (**6**) contain the supplementary crystallographic data for this paper. These data can be obtained free of charge from the Cambridge Crystallographic Data Centre via www.ccdc.cam.ac.uk/data_request/cif.

Supporting Information (see footnote on the first page of this article): Selected NMR spectroscopic data for **1**, **2** and **6**, X-ray data collection, structure solution, refinement, and X-ray diffraction details of compounds **4**–**6**, MTT assay and flow cytometry.

Acknowledgments

This work has been supported by grants from the Fondo de Investigación Sanitaria (FIS) of the Ministerio de Sanidad y Consumo (PI061479), the Red RIS (RD06-0006-0035), the Fundación para la Investigacion y Prevención del SIDA en España (FIPSE) (24632/07), the Micro and Nano Technology of European Network (MNT-ERA NET 2007) (ref. NAN2007-31198-E), the Fundación Caja Navarra and the Comunidad de Madrid (S-SAL-0159-2006) to M. A. M. F., the Micro and Nano Technology of European Network (MNT-ERA NET 2007) (ref. NAN2007-31135-E) and the Fondo de Investigación Sanitaria (PI080222) to R. G. R., and the "Factoria de Cristalización"/Consolider-Ingenio 2010 to M. P. G. S. This work was also supported by the Centro de Investigación Biomédica en RED, Bioingeniería, Biomateriales y Nanomedicina (CIBER-BBN) as an initiative funded by the VI National R&D&i Plan 2008–2011 under the Iniciativa Ingenio 2010, Consolider Program, CIBER Actions and financed by the Instituto de Salud Carlos III with assistance from the European Regional Development Fund. This work was supported by grants from the Consejería de Educación de la Comunidad de Madrid and the Fondo Social Europeo (FSE) for S. G. G. The authors also thank European Cooperation in the Field of Scientific and Technical Research – Short Term Scientific Mission (COST-STSM) (TD0802-05876). The program CU23GP was kindly provided by Prof. Romanelli, University of Florence, Florence, Italy.

[1] D. I. Bernstein, L. R. Satnberry, S. Sacks, N. K. Ayisi, Y. H. Gong, J. Ireland, R. J. Mumper, G. Holan, B. Matthews, T. NcCarthy, N. Bournel, *Antimicrob. Agents Chemother.* **2003**, *47*, 3784–3788.

[2] E. De Clercq, *Clin. Microbiol. Rev.* **1995**, *8*, 200–239.

[3] E. De Clercq, *Met.-Based Drugs* **1997**, *4*, 173–192.

[4] L. Ronconi, P. J. Sadler, *Coord. Chem. Rev.* **2007**, *251*, 1633–1648.

[5] D. E. Bergstrom, L. Xiaoping, T. D. Wood, M. Witvrouw, S. Ikeda, G. Andrei, R. Snoeck, D. Scjols, E. De Clercq, *Antiviral Chem. Chemother.* **2002**, *13*, 185–195.

[6] D. W. Dixon, A. F. Gill, L. Giribabu, A. N. Vzorov, A. B. Alam, R. W. Compans, *J. Inorg. Biochem.* **2005**, *99*, 813–821.

[7] A. N. Vzorov, D. Bhattacharyya, L. G. Marzilli, R. W. Compans, *Antiviral Res.* **2005**, *65*, 57–67.

[8] a) X. Liang, P. J. Sadler, *Chem. Soc. Rev.* **2004**, *33*, 246–266; b) A. Khan, J. Greenman, S. J. Archibald, *Curr. Med. Chem.* **2007**, *14*, 2257–2277; c) A. Khan, G. Nicholson, J. Greenman, L. Madden, G. McRobbie, C. Pannecouque, E. De Clercq, R. Ullom, D. L. Maples, R. D. Maples, J. D. Silversides, T. J. Hubin, S. J. Archibald, *J. Am. Chem. Soc.* **2009**, *131*, 3416–3417.

[9] For some examples of metal complexes as transcriptase reverse, integrase and protease inhibitors, see: a) F. Lebon, N. Boggetto, M. Ledecq, F. Durant, Z. Benatallah, S. Sicsis, R. Lapouyade, O. Kahn, A. Mouithys-Mickalad, G. Deby-Dupont, M. Reboud-Ravaux, *Biochem. Pharm.* **2002**, *63*, 1863–1873; b) O. J. D′Cruz, Y. Dong, F. M. Uckun, *Biochem. Biophys. Res. Commun.* **2003**, *302*, 253–264; c) M. Sechi, A. Bacchi, M. Carcelli, C. Compari, E. Duce, E. Fisicaro, D. Rongolino, P. Gates, M. Derudas, L. D. Al-Mawsawi, N. Neamati, *J. Med. Chem.* **2006**, *49*, 4248–4260; d) B. Courcot, D. Firley, P. Becker, J. M. Gillet, P. Pattison, D. Chernyshov, M. Sghaier, F. Zouhiri, D. Desmaele, J. d'Angelo, F. Bonhomme, S. Geiger, N. E. Ghermani, *J. Phys. Chem. B* **2007**, *111*, 6042–6050; e) M. Kozisek, P. Cígler, M. Lepsik, J. Fanfrlik, P. Rezacova, J. Brynda, J. Pokorná, J. Plesek, B. Grüner, K. Grantz Saskova, J. Vaclavikova, V. Kral, J. Konvalinka, *J. Med. Chem.* **2008**, *51*, 4839–4843.

[10] H. C. Liang, S. K. Das, J. R. Galvan, S. M. Sato, Y. Zhang, L. N. Zakharov, A. L. Rheingold, *Green Chem.* **2005**, *7*, 410–412.

[11] C. A. Grapperhaus, C. S. Mullins, P. M. Kozlowski, M. S. Mashuta, *Inorg. Chem.* **2004**, *43*, 2859–2866.

[12] a) Q. Yu, A. Kandegedara, Y. Xu, D. B. Rorabacher, *Anal. Biochem.* **1997**, *253*, 50–56; b) A. Kandegedara, D. B. Rorabacher, *Anal. Chem.* **1999**, *71*, 3140–3144; c) H. E. Mash, Y.-P. Chin, L. Sigg, R. Hari, H. Xue, *Anal. Chem.* **2003**, *75*, 671–677.

[13] R. K. Henderson, E. Bouwman, A. L. Spek, J. Reedijk, *Inorg. Chem.* **1997**, *36*, 4616–4617.

[14] a) B. J. Hathaway, R. J. Dudley, P. Nicholls, *J. Chem. Soc. A* **1965**, 1845–1848; b) B. J. Hathaway, I. M. Procter, R. C. Slade, A. A. D. Tomlinson, *J. Chem. Soc. A* **1965**, 2219–2223.

[15] H. Kurosaki, H. Koike, S. Omori, Y. Ogata, Y. Yamaguchi, M. Goto, *Inorg. Chem. Commun.* **2004**, *7*, 1229–1232.

[16] E. T. Papish, M. T. Taylor, F. E. Jernigan, M. J. Rodig, R. R. Shawhan, G. P. A. Yap, F. A. Jové, *Inorg. Chem.* **2006**, *45*, 2242–2250.

[17] K. Kurdziel, T. Glowiak, *Polyhedron* **2000**, *19*, 2183–2188.

[18] M. F. Ottaviani, S. Bossmann, N. J. Turro, D. A. Tomalia, *J. Am. Chem. Soc.* **1994**, *116*, 661–671.

[19] H. Beinert, *Coord. Chem. Rev.* **1980**, *33*, 55–85.

[20] a) B.-L. Wu, P. Zhang, Y.-Y. Niu, H.-Y. Zhang, Z.-J. Li, H.-W. Hou, *Inorg. Chim. Acta* **2008**, *361*, 2203–2209; b) T. S. Lobana, I. Kinoshita, K. Kimura, T. Nishioka, D. Shiomi, K. Isobe, *Eur. J. Inorg. Chem.* **2004**, 356–367.

[21] a) R. Fu, S. Hu, X. Wu, *Inorg. Chem.* **2007**, *46*, 9630–9640; b) K. Kimura, T. Kimura, I. Konoshita, N. Nakashima, K. Kitano, T. Nishioka, K. Isobe, *Chem. Commun.* **1999**, 497–498; c) J. M. Plummer, J. A. Weitgenant, B. C. Noll, J. W. Lauher, O. Wiest, P. Helquist, *J. Org. Chem.* **2008**, *73*, 3911–3914.

[22] a) H. Endres, D. Nothe, E. Rossato, W. E. Hatfield, *Inorg. Chem.* **1984**, *23*, 3467–3473; b) C. Fernandes, A. J. Bortolozzi, B. Spoganicz, E. Schwingel, A. Neves, *Inorg. Chim. Acta* **2005**, *358*, 997–1004; c) G. A. Santillan, C. J. Carrano, *Dalton Trans.* **2008**, 3995–4005.

[23] a) M. F. Ottaviani, S. Bossmann, N. J. Turro, D. Tomalia, *J. Am. Chem. Soc.* **1994**, *116*, 661–671; b) M. F.Ottaviani, R. Valluzzi, L. Balogh, *Macromolecules* **2002**, *35*, 5105–5115; c) M. F. Ottaviani, F. Montalti, N. J. Turro, D. Tomalia, *J. Phys. Chem. B* **1997**, *101*, 158–166.

[24] Z. Qiang, C. Adams, *Water Res.* **2004**, *38*, 2874–2890.

[25] G. M. Sheldrick, *SHELXL-97*, *Program for Crystal Structure Refinement*, University of Göttingen, Göttingen, **1997**.

[26] WinGX System: L. J. Farrugia, *J. Appl. Crystallogr.* **1999**, *32*, 837–838.

Received: October 20, 2010
Published Online: February 22, 2011

